May 2007

Assemblies of Carbon Nanotubes and Unencapsulated Sub-10-nm Gold Nanoparticles

Qingling Hang
Purdue University, jgoecker@purdue.edu

Matthew R. Maschmann
Birck Nanotechnology Center, School of Mechanical Engineering, Purdue University, maschmann@purdue.edu

Timothy Fisher
tsfisher@purdue.edu

David B. Janes
Purdue University, david.b.janes.1@purdue.edu

DOI: 10.1002/smll.200600703

Assemblies of Carbon Nanotubes and Unencapsulated Sub-10-nm Gold Nanoparticles

*Qingling Hang, Matthew R. Maschmann, Timothy S. Fisher, and David B. Janes**

The development of assemblies consisting of unencapsulated, sub-10-nm gold particles attached to individual carbon nanotubes (CNTs) with diameters of 2 nm is described. The assemblies are formed on the surface of a porous anodic alumina (PAA) template on which the CNTs (single- or double-walled) are grown by plasma-enhanced chemical vapor deposition. The Au nanoparticles are formed through an indirect evaporation technique using a silicon nitride membrane mask, and diffuse along the PAA surface into the regions containing CNTs. The nanoparticles bind relatively strongly to the CNTs, as indicated by observations of nanoparticles that are suspended over pores or that move along with the CNTs. This approach may provide a new method to functionalize CNTs for chemical or biological sensing and fundamental studies of nanoscale contacts to CNTs.

Keywords:
- carbon nanotubes
- gold
- indirect evaporation
- nanoparticles

1. Introduction

Since the first synthesis of carbon nanotubes (CNTs) in the early 1990s,[1,2] there has been extensive study into the growth of CNTs because of their outstanding physical properties. For instance, laser ablation,[3,4] chemical vapor deposition,[5,6] and plasma enhanced chemical vapor deposition (PECVD)[7] are routinely utilized to produce CNTs. Diodes,[8] field-effect transistors,[9] sensors,[10] and other electronic CNT devices have been widely reported. CNTs represent unique conductors as they provide relatively high effective mobilities even at diameters as small as 1 nm. The quasi one-dimensional (1D) nature of the conductivity in single-walled nanotubes (SWNTs) contributes to their exceptional performance, in part by reducing the amount of small-angle scattering normally found in 2D or 3D conductors.

Assemblies involving CNTs have also been developed[11–13] in order to provide suitable structures for electronic devices and chemical/biological sensing. Studies of electronic devices employing CNTs as channels typically employ large-area contacts using deposition techniques such as evaporation. Depending on the nature of the CNTs and the contact metallization, both Schottky[14] and ohmic[9] contacts have been reported. However, to date there have been few studies on nanoscale contacts to CNTs with well-controlled interfaces. Therefore, it has been difficult to develop a good understanding of the microscopic interaction between metals and CNTs.

For sensing applications, functionalized device structures would enable selective sensors. However, the difficulty in directly functionalizing CNTs, as well as the inability to obtain isolated, bare SWNTs using common bulk synthesis methods, limits the applicability of CNTs as primary elements in sensors.

[*] Dr. Q. Hang, Dr. D. B. Janes
School of Electrical and Computer Engineering
Purdue University
West Lafayette, IN 47907 (USA)
Fax: (+1) 765-494-0811
E-mail: janes@ecn.purdue.edu
Dr. M. R. Maschmann, Prof. T. S. Fisher
Department of Mechanical Engineering
Purdue University
West Lafayette, IN 47907 (USA)

small NANO MICRO

In contrast, it is relatively straightforward to functionalize Au surfaces, including Au nanoclusters. Gold nanoparticles have proven to be versatile in chemical and biological studies. Thiol molecules are used to stabilize gold nanoparticles by covalent Au–S bonds,[15] and they are also used to functionalize DNA to form DNA probes.[16] Therefore, there have been attempts to combine functionalized Au nanoparticles with CNTs in order to improve sensing devices. In one study, 6-nm-diameter Au nanoparticles were first stabilized by tetraoctylammonium bromide, then attached to CNTs.[17] Although this approach does yield Au nanoparticles attached to the CNTs, the encapsulant does not allow intimate contact between the Au and the CNT, and also restricts the availability of sites on the Au nanoparticles for further chemical functionalization. It would be preferable to use unencapsulated nanoparticles, ideally on bare CNTs. However, such gold nanoparticles tend to coalesce into larger gold nanoparticles, as has been demonstrated before by the evaporation of gold onto suspended CNTs.[18] This study involving direct evaporation of metals on suspended SWNTs revealed that evaporated gold formed segments on SWNTs with a nominal thickness of 5 nm and up to 60-nm-diameter gold particles on SWNTs with a nominal thickness of 15 nm. These results indicate that individual atoms of Au (and other metals) have relatively small binding energies to SWNTs, so that incident atoms are mobile on the SWNT until they reach a nucleation site or a larger assembly of Au atoms.

In this paper, we report a technique for forming assemblies consisting of unencapsulated, sub-10-nm Au nanoparticles that are stably bound to bare CNTs with diameters of approximately 2 nm. The closely coupled Au nanoparticles may eliminate the need to chemically modify carbon nanotubes in order to tailor their physical and chemical properties.

2. Results and Discussion

The CNTs were grown using microwave plasma-enhanced chemical vapor deposition (PECVD; see Experimental Section and Figure 1 for details). The growth was catalyzed with a buried iron layer integrated into a porous anodized alumina (PAA) template on a Si substrate. CNTs grown using similar conditions, but using two iron layers in the PAA, were characterized using micro-Raman spectroscopy and high-resolution transmission electron microscopy (HRTEM). The resulting CNTs were observed to be a mix of single-walled and double-walled nanotubes (DWNTs), with diameters of approximately 2 nm.[19] While the single iron layer used in the current experiment may result in a lower percentage of DWNTs, it is believed that the resulting CNTs are of comparable diameter and contain no more than two walls each.

The formation of the Au nanoparticles and docking to the CNTs involves evaporation through a membrane mask, consisting of a suspended, patterned silicon nitride film. The nitride membrane shields the surface of the PAA film from direct exposure to the evaporated Au, except in the patterned windows. However, because of the moderate roughness of the PAA surface and the membrane mask, there was no intimate contact between these surfaces. Therefore, it is possible for Au to diffuse along the PAA surface into the regions that are shielded by the membrane. Of the regions nominally shielded by the nitride film, three distinct regions were observed on the PAA surface, as shown in Figure 2a, at increasing distances from the openings: i) a semicontinuous Au film composed of multiple grains, ii) a transition region in which a sparse coverage of small Au nanoparticles was observed, and iii) a region where negligible Au was observed. The presence of the various regions is attributed to the migration of Au on the surface; as the Au atoms migrate, they also aggregate, forming grains (at large surface coverage) and small nanoparticles (at lower surface coverage). As shown schematically in Figure 2b, within region (ii) the Au nanoparticles are observed on the PAA surface and on the CNTs.

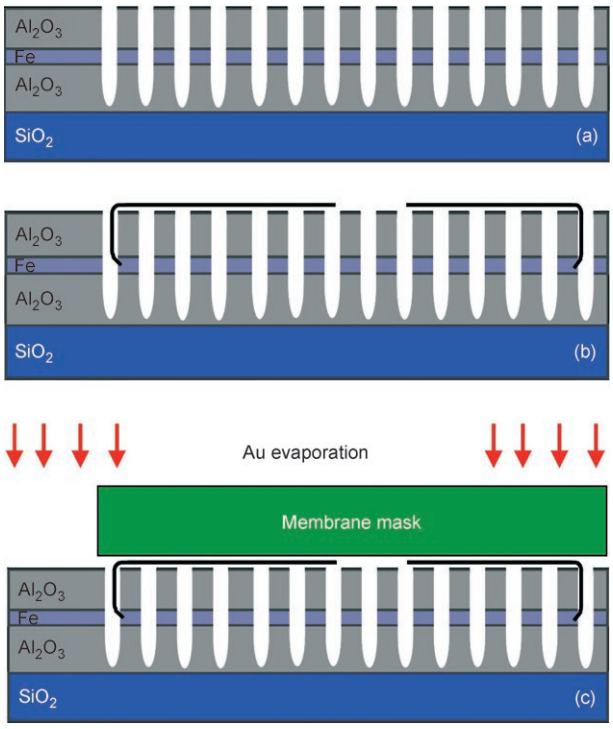

Figure 1. a) Diagram of a cross section of a PAA film with an iron layer as catalyst. The pores are formed by anodization of the Al film, which also anodizes through the Fe layer. b) SWNTs are grown from these pores by PECVD. c) A membrane mask is used during evaporation to pattern a Au film.

Various areas within the three regions were imaged using field-emission scanning electron microscopy (FESEM), as shown in Figure 3. Figure 3a shows an area within region (i), displaying a semicontinuous Au film with aggregated Au islands. Figure 3b shows an area within region (ii) containing two crossed CNTs. Two distinct types of feature are observed on (or near) the CNTs. There are a number of well-defined particles with diameters of approximately 5 nm observed along the CNTs, believed to be Au nanoparticles. In addition, there are somewhat diffuse

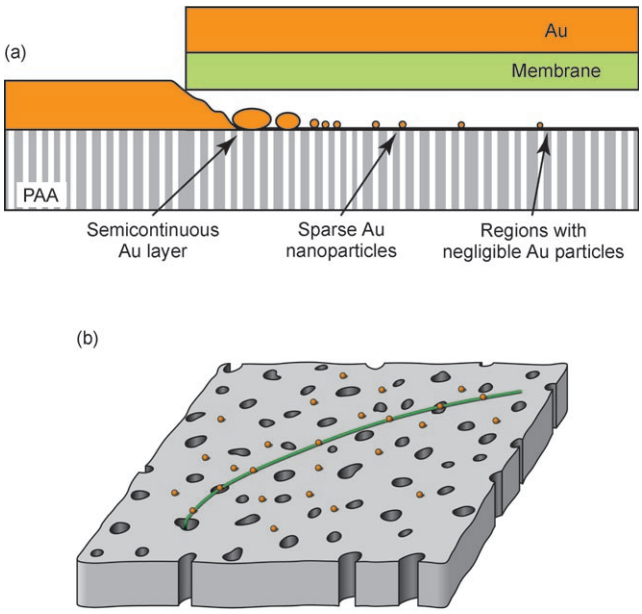

Figure 2. a) Schematic representation of the three regions with different Au particle distribution on the PAA film after Au evaporation through a nitride membrane mask. b) Enlarged view of region (ii), showing one CNT emerging from a pore and growing along the PAA surface. Au nanoparticles diffuse into this region and attach to the CNT.

bright regions with dimensions of 20–40 nm, believed to be due to local charging effects arising during the FESEM imaging. In this case, nanoparticles are observed within the diffuse bright regions. Nanoparticles are also observed elsewhere on the PAA surface, with sizes comparable to those on the CNTs.

In contrast, images taken within region (iii) far from the openings in the membrane mask exhibit diffuse bright features but do not exhibit the ≈5-nm features either on or away from the CNTs. Figure 3c shows CNTs on the PAA surface in an area within region (iii). Two types of CNT are observed. One is shown on the right of Figure 3c; these CNTs are almost smooth wires with few bright areas. Another type is shown in the upper left corner of Figure 3c; this CNT is decorated with several diffuse bright spots. These features are also observed in comparable samples imaged before Au deposition, and therefore are not believed to arise from the deposited Au. The diffuse bright spots observed in both Figure 3b and c may be from a low electrostatic potential compared with the surrounding area,[20] which leads to the emission of more secondary electrons in these regions, resulting in stronger secondary signals. This effect could correspond to spatial variations in the nature of the contact between the CNT and the alumina surface.

In Figure 3b and c (and in subsequent Figures), three-percent backscattered electron (BSE) signals were added to the images in order to reduce specimen-charging effects and to enhance compositional information. This signal corresponds to a wide angle of the emission of backscattered electrons with energies larger than 50 eV and less than the

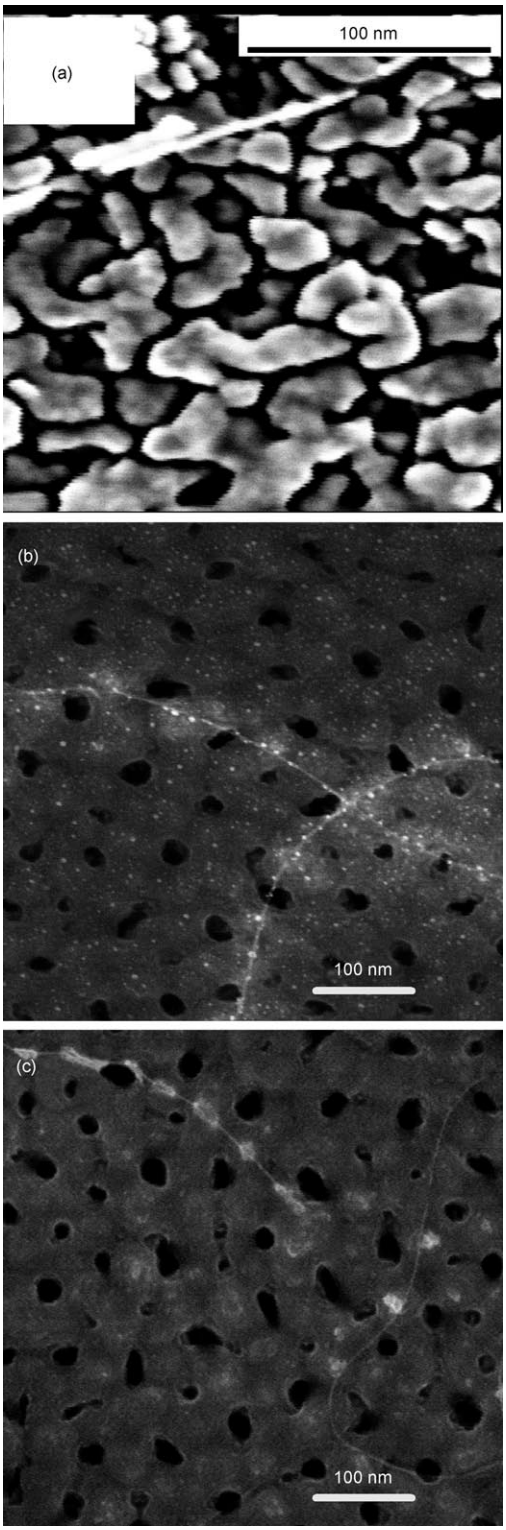

Figure 3. FESEM images of representative areas within the three regions described in Figure 2. a) An area within region (i), showing a semicontinuous Au film on the PAA surface. b) An area from region (ii), showing two crossed CNTs decorated with Au nanoparticles. There are also other gold nanoparticles with sizes comparable to those on CNTs. Diffuse bright spots are also observed along the two tubes. c) An area from region (iii) showing CNTs without Au nanoparticles at the upper left side and along the right-hand side. These CNTs exhibit the diffuse bright spots that are typically observed for CNTs on PAA in samples that have not been exposed to Au.

small NANO MICRO

primary electrons.[21] The three-percent BSE signal does not degrade the resolution significantly; however, it suppresses the effects of local surface electrostatic potential so that the difference between surface potential variations and particles can be appreciable. For the area shown in Figure 3b, the contrast of the ≈5-nm features increased when the BSE signal was added, indicating that these features correspond to a change in composition. However, the ≈20-nm diffuse regions in both Figure 3b and Figure 3c did not change significantly upon addition of the BSE signal, indicating that these regions are likely due to changes in local electrostatic potential distributions associated with charging effects. This observation, along with the observation of the ≈5-nm features on the PAA surface within region (ii) but not in region (iii), leads to the conclusion that the CNTs in region (ii) are decorated with ≈5-nm Au nanoparticles, which formed on the PAA surface and diffused into region (ii).

Figure 4a shows another CNT in region (ii) that is also decorated with ≈5-nm Au nanoparticles. In this image, one of the gold nanoparticles on the CNT is suspended above a 20-nm pore in the PAA film, as indicated by the arrow. This result indicates that the nanoparticle is attached to the CNT, rather than sitting adjacent to the CNT but supported by the surrounding PAA. Under the assumption that the Au nanoparticles diffused into this area along the PAA surface, there are two possible mechanisms that could lead to a nanoparticle suspended over a pore. The first is that the nanoparticle initially contacted the CNT at a location outside of the pore, then diffused along the CNT. There have been reports of selective growth of metal clusters at defect locations on a carbon nanotube,[13] which may indicate differential binding energies at defect sites. It is also possible that the local electrostatic potential distribution could induce motion along the CNT. The second is that CNTs moved along the surface following binding of the gold nanoparticle; this phenomenon will be illustrated in the next section.

Suspended nanoparticles are also observed in regions with larger densities of nanoparticles. Figure 4b illustrates this situation in which a sub-3-nm gold nanoparticle is suspended above the pore, and a relatively high density of gold nanoparticles is observed along the CNT. We left this sample in the SEM chamber for 10 min with the 30 keV beam scanning the area. No appreciable movement of this gold nanoparticle along the CNT was observed, indicating that the particle is stable on the CNT.

Figure 5a depicts an area with two CNTs crossing on the PAA surface, with one passing over pores A and B, another over pores B and C. For clarity, the nanoparticles on the first CNT are highlighted. Figure 5b–f presents a time sequence of images from a cropped region within the area shown in Figure 5a. The overall time interval between the first and last of the images shown in Figure 5 is approximately 6 min. The CNT along A and B is observed to move along the surface in the time interval between Figures 5a and f. Prior to the image shown in Figure 5a, a region of the A–B CNT near pore B, and the Au nanoparticle above pore B, was observed to oscillate between the two edges of the pore at a low frequency of a few Hertz, as observed by successive images. Intermediate images indicate a series of movements as shown in Figure 5a to f, with Figure 5a corresponding to a position close to the initial position and Figure 5f corresponding to a relatively steady-state configuration associated with "roping" of the two CNTs. The presence of the pores in the PAA film provides a local coordinate system for the motion. Through comparison of the relative positions of the nanoparticles in the time sequence of images, it is clear that the Au particles on the CNT move with the CNT, indicating that the Au nanoparticles have a stronger interaction with the CNT than with the PAA surface. The strong mechanical binding between the Au nanoparticles and the CNTs indicates a relatively intimate contact between the two objects, and that the binding energy is larger than the binding energy between the cluster and the

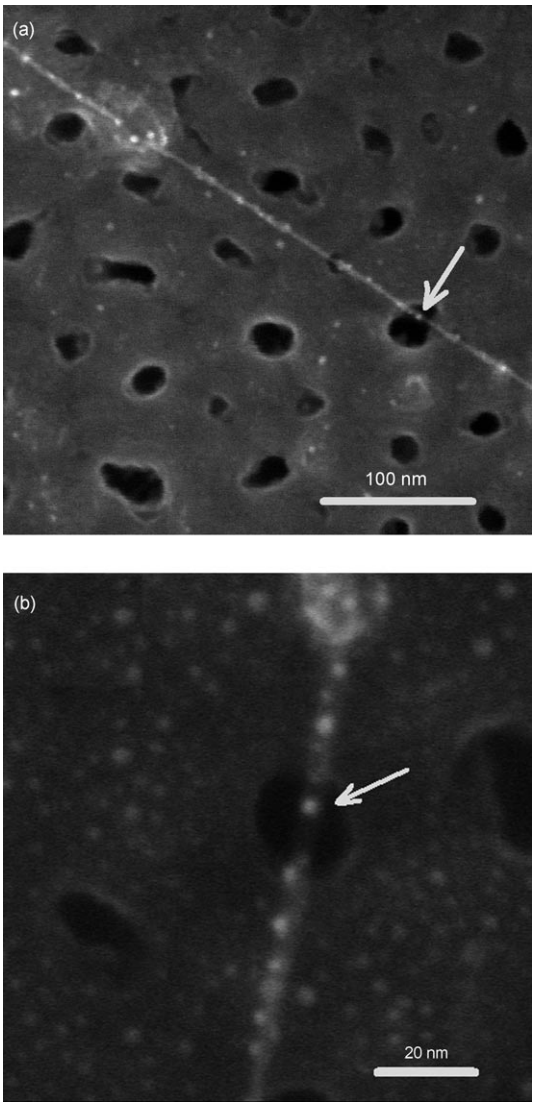

Figure 4. Sub-5-nm gold nanoparticles suspended on the CNTs. a) Sub-5-nm gold nanoparticle indicated by white arrow is on a CNT and above the pore in the PAA film. b) 3-nm gold nanoparticle suspended on a pore by the CNT. This image is from an area with a 10-μm gap with more available gold nanoparticles migrating from the large gold pads.

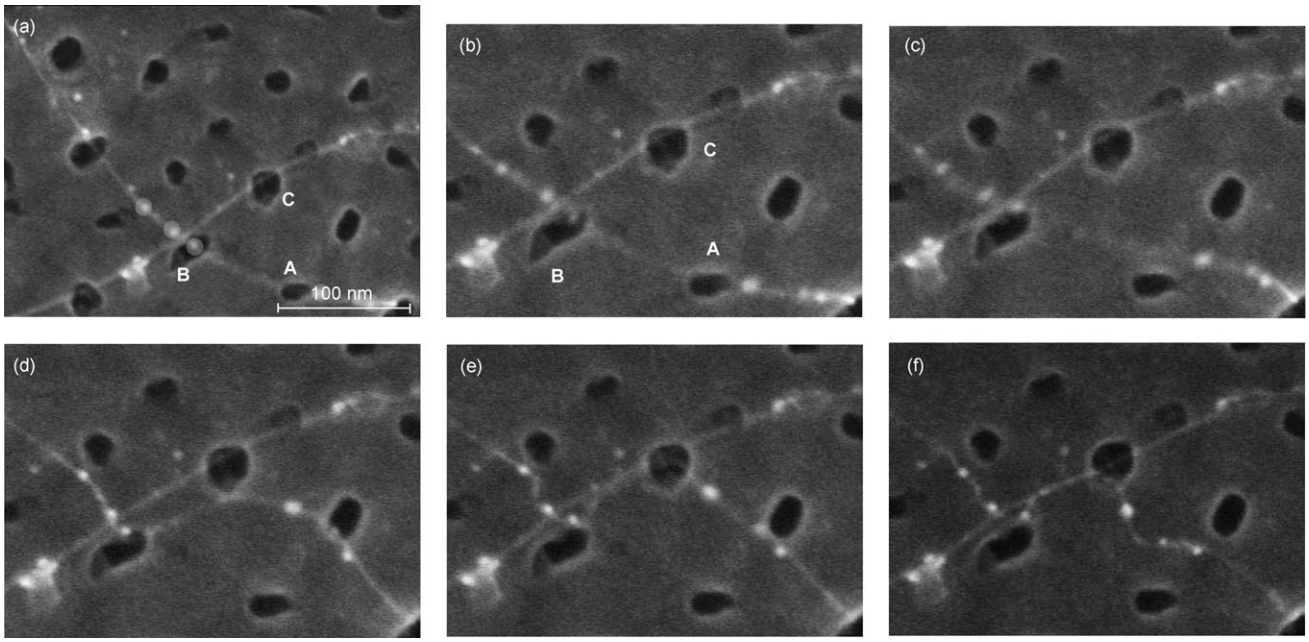

Figure 5. Time-sequence FESEM images of gold nanoparticles on CNT. a) "Initial" state, showing two decorated CNTs on the PAA surface, one initially passed over pores A and B, another passed over pores B and C. Gold nanoparticles on the CNT along A and B are highlighted. The gold nanoparticle over hole B was observed to oscillate from one side of the pore to the other. b–f) Time sequence of images for a cropped portion of the area shown in (a). The movement of one of the CNTs, and the associated nanoparticles, is seen in this time progression of images. In the last two images, the two CNTs appear to be roping in a segment between pores B and C. Following the image shown in (f), the CNTs appear to remain in a relatively steady state.

alumina surface. This behavior is important for realizing a strongly coupled electronic system.

An estimation of the Lennard–Jones (LJ) 12-6 potential between the gold nanoparticles and the graphite surface (parameters for the LJ potential are taken from a previous report[22]) yields a binding energy between one gold atom and one carbon atom of −12.7 meV, about half of the thermal energy at room temperature. This explains why gold atoms tend to migrate and coalesce into either segments or larger clusters in the situation of direct deposition of gold onto suspended CNTs,[18] where the substrate surface temperature was much higher than room temperature. However, the current experiment is different in two important aspects. First, the CNTs are supported on the PAA surface. In addition, the indirect evaporation technique allows the Au to coalesce into nanoparticles before reaching the CNTs in region (ii). Therefore, the appropriate binding energy is that between a Au cluster and a CNT, rather than that of an individual Au atom. An estimation of the LJ potential between a Au particle and a graphite plane was made for a 2.7-nm Au particle, corresponding to the dimensions estimated from Figure 4b. If we assume that the CNT supporting the particle is a SWNT with a diameter of 1.4 nm and assume that the gold atoms encompass the SWNT at one end of the cluster, a binding energy of approximately −5.8 eV is calculated between this gold nanoparticle and the SWNT, which is comparable to the −7.7 eV scaled from a previous report,[23] where gold clusters were treated as truncated octahedra. Compared to gold atoms, the binding of these nanometer-size gold nanoparticles to CNTs is much stronger, thus, the nanoparticles are not mobile enough to approach each other. This result likely explains the fact that gold nanoparticles seldom coalesce to form continuous segments of gold clusters.

Possible applications of the Au/CNT assemblies include nanoscale contacts and chemical sensing. The formation of low-resistance ohmic contacts to CNTs typically requires the deposition of specific metals (e.g., Pd) and subsequent annealing, which may modify the metallurgical interface between the metal and CNT. The use of tightly coupled nanoparticles could allow the development of low-resistance contacts using other metals, and using lower post-processing temperatures, which would be desirable for applications such as flexible electronics. For sensing, the Au nanoparticles can be functionalized (after docking onto the CNTs) in order to provide selectivity to specific target molecules. The charge and/or dipoles associated with the binding of target molecules to the receptors is expected to induce an effective gate field on the nanotube, causing a shift in threshold voltage (as measured using the back gate on the device structure) or inducing an effective access resistance to the channel. The sensitivity of such a sensor device can be estimated by considering the change in surface potential that would be induced on the Au nanoparticle by a molecular binding event and the associated change in molecular charge/dipole. For the case where a molecule binds to a 4-nm Au nanoparticle, with the molecule having one net electronic charge at a separation of 1 nm from the nanoparticle surface, it is estimated that the surface potential of the gold nanoparticle changes by approximately 480 meV. This estimate does not consider the screening of the molecule and assumes that the gold nanoparticle is a perfect conductor. Even considering

NANO MICRO small

the dielectric environment, the surface potential change is still in the range of a few hundred millielectron volts, which is easily detectable for a SWNT field-effect transistor. Therefore, it is possible that a sensing device using an Au/CNT assembly could have sufficient sensitivity to detect a single redox molecule. As an example of molecules that could be detected using such an approach, human mitochondrial glutaredoxin 2 (Grx2), which is related to the maintenance of the homeostasis of cellular redox processes, has been reported to contain a nonoxidizable $[2Fe\text{-}2S]^{2+}$ cluster.[24]

3. Conclusion

A method has been developed to form assemblies of unencapsulated, sub-10-nm gold nanoparticles on isolated 2-nm CNTs. Unlike the case of direct evaporation of Au onto CNTs, defect sites on the CNTs are not necessary in our method of preformed Au nanoparticles. The gold nanoparticles adhere strongly to the CNTs, as evidenced by the observation of nanoparticles suspended above pores and the movement of the assemblies on the PAA surfaces. This effect is consistent with the binding energy between a nanoscale Au cluster and a graphite surface estimated using the Lennard–Jones potential. These assemblies may provide a means to modify the electrical properties of the CNTs without the need of introducing impurities or directly functionalizing the nanotube. Potential applications include selective chemical sensing and nanoscale ohmic contacts.

4. Experimental Section

To form the PAA film, 200 nm of aluminum, 5 nm of iron, and 500 nm of aluminum were successively deposited on an oxidized silicon wafer. The layered stack was anodized at 40 V in 0.3 M oxalic acid at 4 °C to form the modified PAA structure, which included anodization through the iron layer, as shown in Figure 1. CNTs were grown by PECVD at 10 torr, 800 °C surface temperature (monitored by a dual-wavelength pyrometer), 50 sccm H_2, 10 sccm CH_4, and 300 W microwave power for 10 min. Nucleation of CNTs occurred at the iron catalyst layer within the pore, with CNTs emerging at the top of the PAA surface.

Evaporation through a membrane mask was preformed for the formation of the Au nanoparticles and docking to the CNTs. This membrane mask consisted of a suspended, patterned silicon nitride film and utilized a 500-nm-thick nitride film that was deposited by low-pressure chemical vapor deposition (LPCVD) on a silicon substrate. Openings in the membrane mask were realized by etching 50 μm by 50 μm windows in the nitride film, with various spacings, and etching larger openings through the silicon substrate. This mask was then placed in contact with the CNT-covered PAA surface, with the nitride surface facing the PAA. The assembly was transferred to an electron-beam evaporator for deposition of a Au film with a thickness of 320 nm. FESEM was carried out using a Hitachi S4800 microscope.

Acknowledgements

This work was supported by NASA-INAC, under grant NCC 2-1363

[1] S. Iijima, *Nature* **1991**, *354*, 56 – 58.
[2] S. Iijima, T. Ichihashi, *Nature* **1993**, *363*, 603 – 605.
[3] R. Lee, H. Kim, J. Fischer, A. Thess, R. Smalley, *Nature* **1997**, *388*, 255 – 257.
[4] Y. Zhang, H. Gu, S. Iijima, *Appl. Phys. Lett.* **1998**, *73*, 3827 – 3829.
[5] W. Z. Li, S. S. Xie, L. X. Qian, B. H. Chang, B. S. Zou, W. Y. Zhou, R. A. Zhao, G. Wang, *Science* **1996**, *274*, 1701 – 1703.
[6] C. L. Cheung, J. H. Hafner, T. W. Odom, K. Kim, C. M. Lieber, *Appl. Phys. Lett.* **2000**, *76*, 3136 – 3138.
[7] L. C. Qin, D. Zhou, A. R. Krauss, D. M. Gruen, *Appl. Phys. Lett.* **1998**, *72*, 3437 – 3439.
[8] M. Freitag, M. Radosavljevic, Y. Zhou, A. T. Johnson, *Appl. Phys. Lett.* **2001**, *79*, 3326 – 3328.
[9] A. Javey, J. Guo, Q. Wang, M. Lundstrom, H. Dai, *Nature* **2003**, *424*, 654 – 657.
[10] S. Chopra, K. McGuire, N. Gothard, A. M. Rao, A. Pham, *Appl. Phys. Lett.* **2003**, *83*, 2280 – 2282.
[11] R. J. Chen, S. Bangsaruntip, K. A. Drouvalakis, N. W. S. Kam, M. Shim, Y. Li, W. Kim, P. J. Utz, H. Dai, *Proc. Natl. Acad. Sci. USA* **2003**, *100*, 4984 – 4989.
[12] A. Star, J.-C. P. Gabriel, K. Bradley, G. Gruner, *Nano Lett.* **2003**, *3*, 459 – 463.
[13] Y. Fan, B. R. Goldsmith, P. G. Collins, *Nat. Mater.* **2005**, *4*, 906 – 911.
[14] S. Heinze, J. Tersoff, R. Martel, V. Derycke, J. Appenzeller, P. Avouris, *Phys. Rev. Lett.* **2002**, *89*, 106 801 – 106 804.
[15] M. Brust, C. J. Kiely, *Colloids Surf. A* **2002**, *202*, 175 – 186.
[16] N. C. Harris, C. H. Kiang, *Phys. Rev. Lett.* **2005**, *95*, 046 101 – 046 104.
[17] S. Fullam, D. Cottell, H. Rensmo, D. Fitzmaurice, *Adv. Mater.* **2000**, *12*, 1430 – 1432.
[18] Y. Zhang, N. W. Franklin, R. J. Chen, H. Dai, *Chem. Phys. Lett.* **2000**, *331*, 35 – 41.
[19] M. R. Mashmann, A. D. Franklin, P. Amama, D. N. Zakharov, E. A. Stach, T. D. Sands, T. S. Fisher, *Nanotechnology* **2006**, *17*, 3925 – 3929.
[20] T. Brintlinger, Y. F. Chen, T. Duorkop, E. Cobas, M. S. Fuhrer, J. D. Barry, J. Melngailis, *Appl. Phys. Lett.* **2002**, *81*, 2454 – 2456.
[21] J. Goldstein, A. J. Roming, D. Newbury, C. Lyman, P. Echlin, C. Fiori, D. Joy, E. Lifshin, *Scanning Electron Microscopy and X-ray Microanalysis*, Plenum Press, New York, NJ **1992**.
[22] S. Arcidiacono, J. H. Walther, D. Poulikakos, D. Passeron, P. Koumoutsakos, *Phys. Rev. Lett.* **2005**, *94*, 105 502 – 105 504.
[23] W. D. Luedtke, U. Landman, *Phys. Rev. Lett.* **1999**, *82*, 3835 – 3838.
[24] C. H. Lillig, C. Berndt, O. Vergnolle, M. E. Lonn, C. Hudemann, E. Bill, A. Holmgren, *Proc. Natl. Acad. Sci. USA* **2005**, *102*, 8168 – 8173.

Received: December 14, 2006
Published online on May 8, 2007

